Dipolar spin echoes in magnetic resonance force microscopy

C. L. Degen,* Q. Lin, and B. H. Meier
Physical Chemistry, ETH Zurich, CH-8093 Zurich, Switzerland
(Received 22 May 2006; published 21 September 2006)

Limits for extending the coherence lifetime in force detected NMR spectroscopy are explored using time suspension pulse sequences based on the "magic echo." Two micron-sized single crystals of KPF_6 and $(NH_4)_2SO_4$ were used for demonstration, where a typical experiment measured signals of $\sim 10^{14}$ spins from a ~ 0.8 μm wide imaging slice. By studying the decay of the dipolar echo maximum it is demonstrated that spectral linewidths of 1.1 kHz collected from a 100 kHz wide frequency slice can be obtained, extending the coherence lifetime for both samples by an order of magnitude.

DOI: 10.1103/PhysRevB.74.104414 PACS number(s): 76.60.Lz, 68.37.Rt, 76.60.Pc

Mechanical detection of nuclear magnetic resonance (MRFM) has resulted in significant increases in the detection sensitivity of nuclear spin signals.[1–3] The method operates within a range of 10^8 to 10^{15} nuclear spins permitting the study of micrometer-scaled objects, a regime in which conventional inductive detection techniques become sensitivity limited. The large field gradients inherent to the mechanical detection scheme can exceed 10^5 T/m and allow for magnetic resonance imaging on solid materials with nanometer scale resolution.[4]

Recent work has demonstrated that mechanical spin detection can be combined with NMR spectroscopy to extend localized spectroscopy to the micrometer and nanometer scale. Despite the presence of the strong field gradient, dipolar spectra with decent resolution have been observed,[5] and quadrupolar coupling parameters were used for image contrast in nutation spectroscopy.[6] Very recently, magnetic double resonance has been used in conjuction with MRFM demonstrating that <1 kHz wide lines can be obtained for ^{31}P spins in KPF_6 by heteronuclear decoupling techniques.[7] Here we consider the slightly different problem of obtaining narrow linewidths in samples containing abundant, high-γ nuclei such as ^{1}H and ^{19}F, where homonuclear spin-spin couplings often form the major contribution to the spectral linebroadening. Removing such contributions is an essential prerequisite for high resolution in modern solid state NMR spectroscopy, and represents the main topic of this experimental study.

Magic echo[8–10] and time suspension[11,12] pulse sequences are established tools to extend the lifetime of the transverse magnetization by eliminating the dipole-dipole interactions and, in the case of time suspension, also the chemical-shift or field-inhomogeneity contributions to the signal decay. The classical "magic echo" reverses the dipolar decay of the free induction decay (FID) by an effective reversal of the preceding time evolution.[8,10,13]

Here, we explore the limits of line narrowing in MRFM detected spectroscopy. Removing the dominant homonuclear dipolar interactions not only forms a necessary condition to obtaining high spectral resolution in ^{1}H and ^{19}F rich samples, the remaining natural linewidth can also provide information about dynamic random processes and spin-diffusion or chemical diffusion processes. Additionally, magic echo-type sequences have been applied in conventional micro imaging,[14] and have been suggested for Fourier imaging techniques in the context of MRFM (Ref. 15).

Echo formation is induced by a sign change of the dipolar Hamiltonian.[10] Defocusing of the spin coherence takes place during time τ_1 in the rotating frame while a radio-frequency (rf) field is applied on resonance. If the rf field is sufficiently strong (that is, the rf amplitude $\nu_1 \gg M_2^{1/2}$, where M_2 is the second moment of the resonance line) the unperturbed dipolar Hamiltonian H_D is scaled to

$$H_D^{rf} = s(\theta_{eff})H_D = \frac{1}{2}(3\cos^2\theta_{eff} - 1)H_D, \qquad (1)$$

where the scaling factor $s(\theta_{eff})$ depends on the direction of the effective magnetic field vector.[10] Specifically, the scaling factor is $s=-1/2$ for on-resonance irradiation ($\theta_{eff}=90°$). The defocusing period is followed by a refocusing time τ_2 during which the unperturbed dipolar Hamiltonian H_D is active ($s=1$) and thus, when $\tau_2=\frac{1}{2}\tau_1$, an echo appears.

Two species of nuclear spins were studied. In one case, the ^{19}F spins in a $\sim 60\times 60\times 35$ μm^3 sized single crystal of KPF_6 were probed. We also investigated protons in $(NH_4)_2SO_4$, using a single crystal of similar dimensions $\sim 40\times 40\times 40$ μm^3. The samples were attached to the tips of commercial silicon nitride cantilevers (Veeco Inc.)[16] and measured in high vacuum and at room temperature using a polarizing field corresponding to ~ 270 MHz proton frequency.[5,7] Although the crystals contain $\sim 3\cdot 10^{15}$ spins each, only $\sim 1\cdot 10^{14}$ spins in a thin slice, typically 1 μm wide, are excited due to the presence of the strong ~ 2700 T/m field gradient.

Figure 1 shows an example of the buildup and decay of a magic echo measured on the ^{19}F spins in the KPF_6 sample. MRFM samples the transient point by point, thus each τ_1 value corresponds to a different experiment. Spectral information is encoded and stored in the magnitude of the magnetization M_z in the indirect "encoding" dimension, while the direct "detection" dimension is used to measure M_z and contains information on spatial position and number of spins in the image slice (see Fig. 2). The information stored in M_z is often persistent on the time scale of the spin-lattice relaxation time T_1, so that encoding and detection may be separated for comparably long durations. Given the instrumental capacity, the time window could be used to switch off the

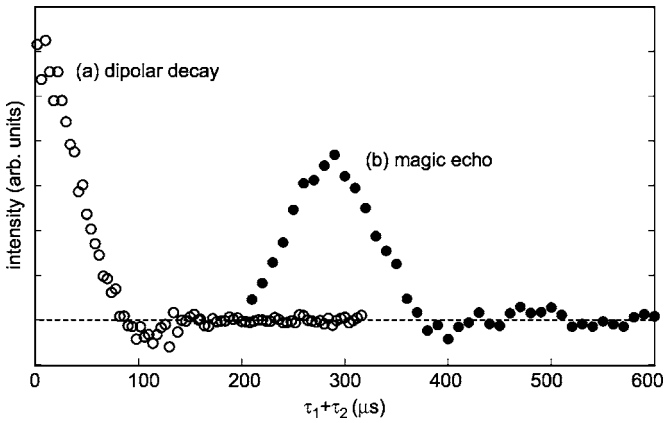

FIG. 1. Dipolar decay (open circles) and magic echo (closed circles) of $\sim 2 \cdot 10^{14}$ ^{19}F spins in KPF_6. Single shot detection limit is $\sim 3 \cdot 10^{12}$ protons equivalent. A defocusing time $\tau_1 = 200$ μs, a nutation rf field strength $\nu_1 = 100$ kHz, and a resonant slice width $\Delta\nu = 100$ kHz were used for the echo. The spatial slice width Δz relates to $\Delta\nu$ via the field gradient G, $\Delta z = 0.8\Delta\nu(\gamma G)^{-1}$, where γ is the gyromagnetic ratio and hence $\Delta z \sim 0.8$ μm. The two measurements were averaged over four transients and required ~ 20 min of acquisition time.

field gradient, and would enable the encoding of spectral information in a homogeneous magnetic field.[17] In our experiments a delay time τ_d between the two periods was introduced because the hard rf pulses excited the cantilever. By waiting τ_d the oscillations were allowed to decay before mechanical detection started.[18] To further reduce spurious resonator excitation caused by rf pulsing, we also employed a two-step phase-cycling protocol. The magnetization was inverted prior to every other experiment and the transients subtracted, leaving out the desired spin signal. This eventually allowed us to reach thermal noise limited detection of the magnetic force signal.

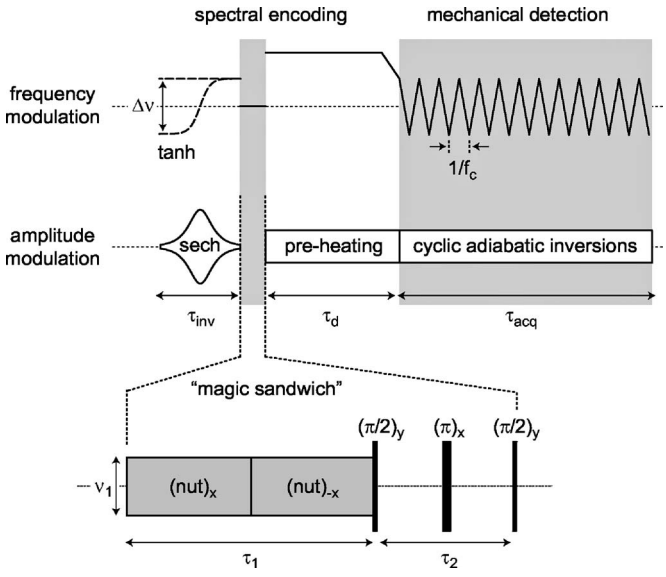

FIG. 2. Pulsing scheme used for all experiments. Typical rf field strengths were 210 kHz (pulses, black), 30–100 kHz (nutation, gray), and 20 kHz (spin lock, white). The duration of a $\pi/2$-pulse was 1.2 μs and required ~ 100 W rf power (details cf. Ref. 7). Inversion time was $\tau_{inv} = 5$ μs, dead time $\tau_d = 300$ ms, and acquisition time $\tau_{acq} = 3$ s. f_c denotes the cantilever frequency (Ref. 16). A selective sech/tanh inversion (dashed line) performed every second acquisition was used for phase cycling. The magic sandwich pulse sequence is explained in the text.

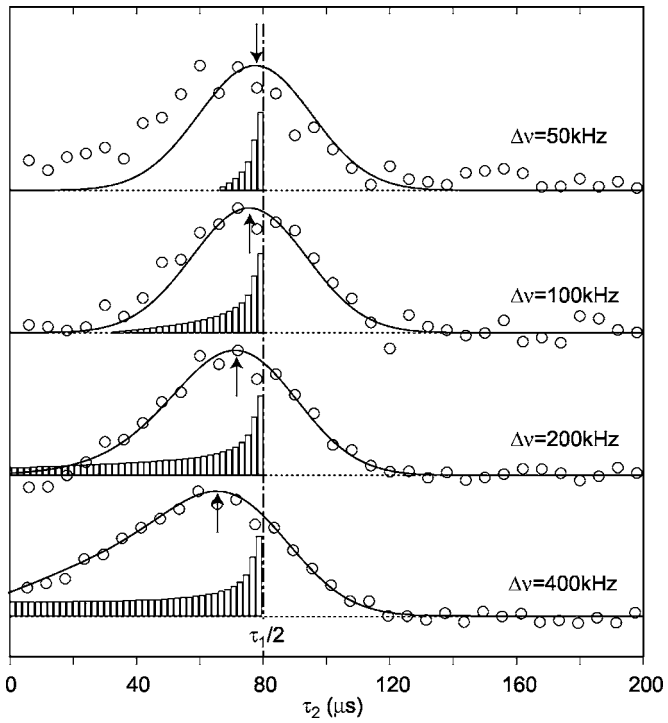

FIG. 3. Influence of field inhomogeneities on magic echo formation in the $(NH_4)_2SO_4$ sample investigated for resonant slice widths between 50 and 400 kHz. A rf field strength of $\nu_1 = 100$ kHz was used together with a defocusing time of $\tau_1 = 160$ μs. The bars represent a histogram of the expected echo maximum positions of all spins in the slice, weighted by the offset dependence of the detection sequence. The solid line further includes the dipolar linewidth and the excitation bandwidth of rf pulses. Arrows indicate the shift of the echo maximum with respect to $\tau_1/2 = 80$ μs. All curves are normalized to the respective maximum value.

Spin encoding in the "magic sandwich" was started with a nutation period of duration τ_1 during which the spins evolved under the influence of the scaled Hamiltonian H_D^{rf} (see Fig. 2).[8–10] Inhomogeneities in the rf field of the coil were compensated by switching the phase by 180° after $\tau_1/2$. The magnetization vector—which resided in the yz plane after τ_1—was then flipped into the xy plane by a first $\pi/2$-pulse, initiating the free coherent evolution under the unperturbed Hamiltonian H_D for a time τ_2. Finally, the resulting magnetization was stored in detectable M_z polarization by a second $\pi/2$ pulse. Rapid dephasing of the coherence due to the presence of the field gradient was prevented by applying a π pulse in the middle of the τ_2 evolution period.

Force signals were collected from all spins in the resonant slice and had a rather wide range of Larmor frequencies. The behavior of the pulse sequence at larger offsets therefore limited the maximum allowed slice width $\Delta\nu$. Figure 3 dis-

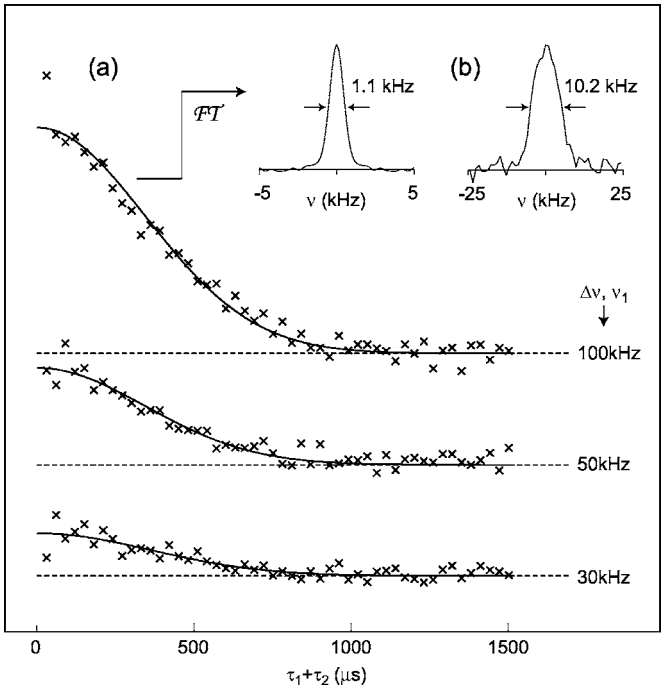

FIG. 4. Decay of the echo maximum in KPF_6 for three different rf field strengths ν_1. The frequency slice width was adjusted such that $\Delta\nu=\nu_1$. The solid lines represent Gaussian fits with $\sigma=304\pm16$ μs, $\sigma=312\pm31$ μs, and $\sigma=318\pm47$ μs from top to bottom, respectively. The insets show the spectra of maximum of the echo decay [$\nu_1=100$ kHz] on the left, and the usual dipolar decay taken from Fig. 1(a) on the right. The linewidth is improved by a factor of ten.

plays two critical issues which are related to the scaling factor $s(\theta_{\text{eff}})$ in the dipolar Hamiltonian under rf excitation H_{D}^{rf} [Eq. (1)]. Since the effective field angle θ_{eff} is at 90° only for a fraction of spins located in the center of the slice, the scaling factor is $s>-0.5$ for most spins across the resonant slice. Consequently a distribution of echoes appears at times $\tau_2<\frac{1}{2}\tau_1$, resulting in an apparent shift and an asymmetric envelope of the echo transient (Fig. 3). The shift is also proportional to the time τ_1 spent on nutation, long echo times are therefore critical. From the results in Fig. 3 we concluded that rf strengths during nutation ν_1 should be at least one times the modulation width $\Delta\nu$ in the present experiments.

Finally, the finite bandwidth of the hard $\pi/2$, π pulses and the details of the modulation scheme must be considered. They can be expressed by a distribution function that relates the force contribution of a certain spin to its Larmor offset Ω, and usually gives the largest weight to the spins in the center of the slice where $|\Omega|$ is small.[19]

In a second set of experiments the signal decay under time suspension was examined, with the goal of extending the signal lifetime as much as possible, and in order to explore the prospects of this method for future high-resolution MRFM spectroscopy experiments. For this purpose, a series of echo maxima was recorded as depicted in Fig. 4(a) where $\tau_2=\frac{1}{2}\tau_1$. This corresponds to a situation where all dipole-dipole interactions and, due to the Hahn-echo during laboratory frame evolution, also the chemical shift, field inhomogeneity and—to a great extent—heteronuclear contributions to the signal decay are eliminated. The decay was measured at three different nutation pulse amplitudes for both samples. Compared to the free dipolar decay from Fig. 1(a), the lifetime of the coherent evolution is extended by an order of magnitude. In the spectral domain [Fig. 4(b)] this corresponds to a decrease in linewidth from 10.2 kHz (the normal dipolar linewidth of KPF_6, in accordance with Ref. 20) to 1.1 kHz for the KPF_6 sample. For the $(NH_4)_2SO_4$ sample a similar decrease from 20 to 2.0 kHz was found (data not shown).

The transients are well described by Gaussians and do not depend on the nutation rf amplitude ν_1 within the accuracy of the fit. This is not so obvious, as the quality of echo formation is expected to depend on rf field strength due to higher order dipolar terms neglected in the zeroth order rotating frame Hamiltonian H_{D}^{rf} [Eq. (1)]. Residual dipolar couplings from higher order terms scale inversely with ν_1, and a dependence of the signal decay on ν_1 is an indication for a residual dipolar broadening mechanism. We do not observe such a dependence, and also the second moment of the fluorine resonance is relatively small ($M_2^{1/2}=4.1$ kHz) due to free rotations of the PF_6^- groups in the crystal.

Other contributions to the linewidth possibly stem from residual heteronuclear spin-spin couplings between ^{19}F and ^{31}P, from imperfections in the pulse sequence (in particular the long nutation pulses), or from intrinsic stochastic processes in the sample.[21] For the latter, however, an exponential rather than Gaussian decay is usually observed.

It is also possible that the mechanical stability of the MRFM operating with very large field gradients plays a critical role in the decay of transient spin signals. Due to vibrations of the cantilever-mounted sample some fluctuations in the polarizing B_0 field are always present, and have shown for example to accelerate the longitudinal relaxation under certain conditions.[22] Thermal tip motion for our experiments are on the order of $z_{\text{rms}}\sim0.1$ nm and thus induce B_0 fluctuations in the order of $z_{\text{rms}}\gamma G\sim12$ Hz, where $G=2700$ T/m is the field gradient and γ the gyromagnetic ratio. Linewidth contributions stemming from thermal tip vibrations are therefore minute. It is, however, possible that the much stronger oscillations excited by rf pulses lead to substantial field variations and are responsible for an incomplete refocusing of the Hahn echo during τ_2. Some additional linebroadening connected to the field gradient may therefore be present. Finally we note that although thermal tip motion induced fluctuations are minute in our study, they could become limiting in future experiments when very soft cantilevers that exhibit higher rms motion are employed on materials with very sharp resonance lines.

In this study we have shown that magic echoes provide a useful tool to narrow dipolar broadened resonance lines in the context of mechanically detected NMR spectroscopy. Two micron-sized single crystals of KPF_6 and $(NH_4)_2SO_4$ were used for demonstration, where a typical experiment collected signals from $\sim10^{14}$ spins from a ~0.8 μm wide imaging slice. Under time suspension signal decay is slowed down by an order of magnitude compared to the dipolar decay for both samples, reaching linewidths down to 1.1 kHz. This demonstrates that magic echoes can form a

valuable tool for high-resolution MRFM spectroscopy because of their compatibility with chemical shift resolution.

The authors thank A. Hunkeler and U. Meier for their work on the setup and M. Hronska for the good atmosphere in the office. We acknowledge financial support from the ETH Zurich, the Schweizerischer Nationalfonds (SNF), and the Kommission für Technologie und Innovation (KTI).

*Present address: IBM Research Division, Almaden Research Center, 650 Harry Road, San Jose, California 95120, USA. Electronic address: degen@nmr.phys.chem.ethz.ch

[1] J. A. Sidles, Appl. Phys. Lett. **58**, 2854 (1991).

[2] D. Rugar, O. Züger, S. Hoen, C. S. Yannoni, H.-M. Vieth, and R. D. Kendrick, Science **264**, 1560 (1994).

[3] H. J. Mamin, R. Budakian, B. W. Chui, and D. Rugar, Phys. Rev. B **72**, 024413 (2005).

[4] D. Rugar, R. Budakian, H. J. Mamin, and B. W. Chui, Nature (London) **430**, 329 (2004).

[5] C. L. Degen, Q. Lin, A. Hunkeler, U. Meier, M. Tomaselli, and B. H. Meier, Phys. Rev. Lett. **94**, 207601 (2005).

[6] R. Verhagen, A. Wittlin, C. W. Hilbers, H. van Kempen, and A. P. M. Kentgens, J. Am. Chem. Soc. **124**, 1588 (2002).

[7] Q. Lin, C. L. Degen, M. Tomaselli, A. Hunkeler, U. Meier, and B. H. Meier, Phys. Rev. Lett. **96**, 137604 (2006).

[8] W. K. Rhim, A. Pines, and J. S. Waugh, Phys. Rev. Lett. **25**, 218 (1970); W. K. Rhim, A. Pines, and J. S. Waugh, Phys. Rev. B **3**, 684 (1971).

[9] K. Takegoshi and C. A. McDowell, Chem. Phys. Lett. **116**, 100 (1985).

[10] C. P. Slichter, *Principles of Magnetic Resonance* (Springer, New York, 1996).

[11] H. M. Cho, C. J. Lee, D. N. Shykind, and D. P. Weitekamp, Phys. Rev. Lett. **55**, 1923 (1985).

[12] S. Matsui, A. Uraoka, and T. Inouye, J. Magn. Reson., Ser. A **120**, 11 (1996).

[13] H. Schneider and H. Schmiedel, Phys. Lett. **30A**, 298 (1969).

[14] S. Hafner, D. E. Demco, and R. Kimmich, Meas. Sci. Technol. **2**, 882 (1991).

[15] J. G. Kempf and J. A. Marohn, Phys. Rev. Lett. **90**, 087601 (2003).

[16] Loaded cantilever eigenfrequencies were $f_c = 875$ Hz and $f_c = 1564$ Hz for the KPF_6 and $(NH_4)_2SO_4$ sample, respectively. Spring constant was 0.01 N/m. Feedback damping was applied to reduce the quality factor from $Q \sim 10{,}000$ (in vacuum) to $Q_{cl} \sim 50$. Further details are given in Ref. 5.

[17] L. A. Madsen, G. M. Leskowitz, and D. P. Weitekamp, Proc. Natl. Acad. Sci. U.S.A. **101**, 12804 (2004).

[18] Delay times τ_d are limited both by the spin-lattice relaxation time T_1 and the cantilever ring-down time τ_c, $\tau_c \ll \tau_d \ll T_1$. In our experiments $\tau_c = 2Q_{cl}/\omega_c \sim 10$ ms using feedback damping on the cantilever, and $T_1 = 6.1$ s (for KPF_6) and $T_1 = 4.1$ s [for $(NH_4)_2SO_4$], respectively.

[19] The slice distribution function for triangular frequency modulation is approximatively given by

$$p(\Omega) \propto \begin{cases} \cos(\pi\Omega/2\Delta\nu) & \text{if } |\Omega| < \Delta\nu/2 \\ 0 & \text{otherwise.} \end{cases}$$

Taking also the rf pulse sequence into account, a good agreement with both simulations and experiments was found for $p \propto \cos^{\alpha}(\cdots)$, $\alpha \sim 8$.

[20] G. R. Miller and H. S. Gutowsky, J. Chem. Phys. **39**, 1982 (1963).

[21] M. Mehring, *Principles of High Resolution NMR in Solids*, 2nd ed. (Springer, Berlin, 1983).

[22] B. C. Stipe, H. J. Mamin, C. S. Yannoni, T. D. Stowe, T. W. Kenny, and D. Rugar, Phys. Rev. Lett. **87**, 277602 (2001).